MINIMUM-FUEL, TWO-IMPULSE, SOFT LUNAR LANDING ORBITS

prepared for

NATIONAL AERONAUTICS AND SPACE ADMINISTRATION

by

Carlos R. Cavoti

Contract NAS 9-5550

September 1966

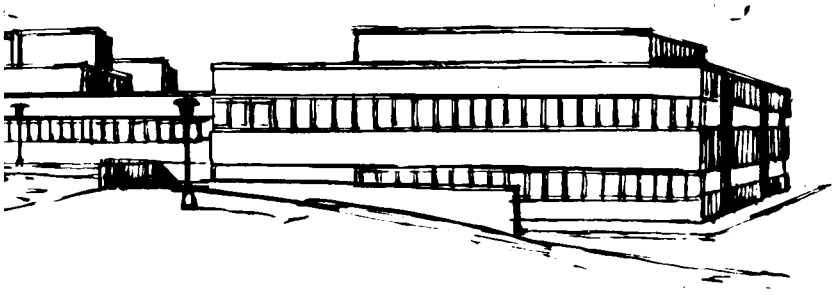

Space Sciences Laboratory
Missile and Space Division
GENERAL ELECTRIC COMPANY
Philadelphia, Pa.

MINIMUM-FUEL, TWO-IMPULSE SOFT LUNAR LANDING-ORBITS

Report
September 1966
Contract NAS 9-5550

Prepared for
National Aeronautics and Space Administration
Manned Spacecraft Center
Houston, Texas

Prepared by
Carlos R. Cavioti
Space Sciences Laboratory
General Electric Company
Philadelphia, Pa.

ABSTRACT

The problem of minimum-fuel-consumption soft lunar landing trajectories is here considered. The trajectories discussed involve two impulses. The boundary conditions are arbitrary.

Practical closed-form expressions for the impulse conditions of useful geometrical meaning are derived. Such expressions are particularly suitable for the formulation of the optimum problem using the method of undetermined Lagrange multipliers.

The necessary conditions for a minimum-fuel-consumption soft lunar landing are derived for both free-range and given-range problems.

The method of numerical solution and several applications are discussed. The basic characteristics of the landing trajectories are analyzed using the expressions derived. Numerical solution shows that, among all the free-range optimum trajectories starting at different points on a given elliptical orbit around the moon, the trajectory starting with a tangential retro-impulse at the apogee affords an absolute minimum fuel consumption. Due to the boundary conditions imposed, a theoretical analysis shows that the transfer orbit can not be of the Hohmann type. Although, depending on the initial orbit assumed, the transfer may closely approximate the Hohmann type.

TABLE OF CONTENTS

LIST OF SYMBOLS

e	Eccentricity
k	Universal gravitational constant
m	Mass of the vehicle
M	Mass of the moon
r	Radius
V	Velocity
z	Dimensionless velocity
α	Dimensionless mass-flow
β	Mass-flow
γ	Central angle
δ	Direction of the impulse
λ	Lagrange multiplier
θ	Angle of attitude
τ	Dimensionless time
ρ	Dimensionless radius
μ	Dimensionless mass
η	Range

Superscripts

$$\dot{(\cdots)} = \frac{d}{dt}(\cdots)$$

$$(\cdots)' = \frac{d}{d\tau}(\cdots)$$

Subscripts

R	Reference value
i	Initial
f	Final
1	Point 1
2	Point 2

1. EQUATIONS OF MOTION - IMPULSIVE SOLUTIONS

It is assumed that a vehicle of mass m is subject to the inverse-square gravitational force field of a uniform, spherical, attracting body of mass M, and to a propulsive force T of arbitrary direction. The forces acting on the vehicle and coordinate system of reference are shown in Figure 1.

Referring the motion of the mass-point vehicle m (Figure 1) with respect to the intrinsic relative system associated with the tangent and normal ($\bar{u}_t$ and $\bar{u}_n$) to the trajectory, the following kinematic and dynamic (linear momemtum) equations are obtained:

$$\dot{r} - V \sin\theta = 0, \tag{1}$$

$$r\dot{\gamma} - V \cos\theta = 0, \tag{2}$$

$$m\dot{V} - \beta V_e \cos(\delta - \theta) + \frac{k M m}{r^2} \sin\theta = 0, \tag{3}$$

$$m\left(V\dot{\theta} - \frac{V^2 \cos\theta}{r}\right) - \beta V_e \sin(\delta - \theta) + \frac{k M m}{r^2} \cos\theta = 0, \tag{4}$$

$$\dot{m} + \beta = 0. \tag{5}$$

The last equation defines the mass-flow of the rocket engine. Thus, the thrusting force is expressed $T = \beta V_e = -\dot{m} V_e$. Here, V_e is the velocity of the burned gases through the exit section of the rocket engine.

To the extent of writing the equations of motion in dimensionless form - which is more convenient for numerical applications - we introduce now the following variables (R = reference constant values):

$$V_R = \left(k \frac{M}{r_R}\right)^{1/2}, \quad z = \frac{V}{V_R}, \quad \tau = \frac{t\, k\, M}{r_R^2\, V_R},$$

$$\rho = \frac{r}{r_R}, \quad v_e = \frac{V_e}{V_R}, \quad \mu = \frac{m}{m_i},$$

$$\alpha = \frac{\beta\, r_R}{m_i\, V_R}.$$

Since the central attracting body is assumed to be the moon, the radius of reference to be considered is the radius of the moon (i.e., $r_R = r_\ell$).

Introducing the previous dimensionless variables in Eqs. (1) to (5), recalling that $\frac{d}{dt}(\cdots) = \frac{kM}{r_R^2 V_R}(\cdots)$ and using a prime to denote total differentiation with respect to the dimensionless time τ, we derive

$$\rho' - z \sin\theta = 0 , \tag{6}$$

$$\gamma' - \frac{z \cos\theta}{\rho} = 0 , \tag{7}$$

$$z' - \frac{\alpha v_e}{\mu} \cos(\delta - \theta) + \frac{\sin\theta}{\rho^2} = 0 , \tag{8}$$

$$\theta' + \left(\frac{1}{z\rho^2} - \frac{z}{\rho}\right) \cos\theta - \frac{\alpha v_e}{\mu z} \sin(\delta - \theta) = 0 , \tag{9}$$

$$\mu' + \alpha = 0. \tag{10}$$

In general, these equations must be integrated numerically in order to determine the powered trajectory of the vehicle.

The study of the trajectory of vehicles powered by high-thrust rocket engines, however, may be substantially simplified using an approximate model of practical value. If the powered periods of the flight are of small duration, as compared to the total transfer time, then one may replace the powered sub-arcs by impulses. Such impulses take place in zero-time and produce an instantaneous change in mass, velocity and angle of attitude of the vehicle. As a result of this approximation the equations of motion may be integrated in closed-form along the powered sub-arcs, thus leading to a significant analytical simplification of the problem. This solution is particularly advantageous in order to conduct comparative studies in which the relative merits of a number of trajectories must be analyzed. Such is precisely our interest in this paper, since-among all lunar soft landing trajectories satisfying given boundary-conditions - we want to determine that trajectory which affords a minimum for the fuel consumption.

The impulsive solution has been previously applied by several authors within the context of a different analytical formulation than that used in this paper. As we will see in the following our formulation of the equations of motion [Eqs. (6) to 10)], referred to the Eulerian intrinsic system ($\bar{u}_t$; $\bar{u}_n$), leads to a closed-form solution of simple physical interpretation which is readily applicable to a new, ample formulation of the optimum problem, using the method of undetermined Lagrange multipliers.

Since the impulse implies the instantaneous burning in a finite amount of propellant, this means that analytically in our equations $\alpha \to \infty$. Thus, eliminating the independent variable τ (dimensionless time) and taking the limit $\alpha \to \infty$ we can obtain the differential expressions of the impulse from the equations of motion. In fact, making the ratios of Eq. (8) and Eq. (10), and Eq. (9) and Eq. (10), after taking the limit $\alpha \to \infty$ we obtain

$$\frac{dz}{d\mu} = - \frac{v_e}{\mu} \cos (\delta - \theta) \quad , \tag{11}$$

$$\frac{d\theta}{d\mu} = - \frac{v_e}{\mu z} \sin (\delta - \theta) \quad , \tag{12}$$

Eqs. (11) and (12) are the differential expressions relating the changes in velocity (z), angle of attitude (θ) and mass (μ) through the impulse.

Eliminating the variable μ from Eqs. (11) and (12) we derive now

$$d \, \mathrm{Ln} \, z = \frac{d\theta}{\tan (\delta - \theta)} \tag{13}$$

Since the angle of orientation of the thrust (δ) is constant through the impulse, Eq. (13) is integrable in closed-form leading to

$$z \sin (\delta - \theta) = C_1 = \text{const.} \tag{14}$$

Now, Eq. (11) implies

$$d \, \mathrm{Ln} \, \mu + \frac{dz}{v_e \cos (\delta - \theta)} = 0 \, , \tag{15}$$

and, since from Eq. (13)

$$dz = z \frac{d\theta}{\tan(\delta - \theta)} \tag{16}$$

then

$$d \operatorname{Ln} \mu + z \frac{d\theta}{v_e \sin(\delta - \theta)} = 0 . \tag{17}$$

Eqs. (14) and (17), after eliminating z, lead to

$$d \operatorname{Ln} \mu + \frac{C_1 \, d\theta}{v_e \sin^2(\delta - \theta)} = 0 , \tag{18}$$

which is readily integrable to

$$\operatorname{Ln} \mu + \frac{C_1}{v_e} \cot(\delta - \theta) = C_2 , \tag{19}$$

and with the help of Eq. (14) reduces to

$$\operatorname{Ln} \mu + \frac{z}{v_e} \cos(\delta - \theta) = C_2 = \text{const.} \tag{20}$$

Eqs. (14) and (20) give the set of closed-form expressions describing the impulse. For any given direction δ of the impulse the values of the velocity z and angle of attitude θ are readily obtained from Eqs. (14) and (20) depending on the amount of fuel burned (or, what is equivalent, the mass of the vehicle before and after the impulse.

Eq. (14) geometrically implies that through the impulse the vector velocity rotates with its free-end following a parallel to the direction of the vector T. This condition is shown in Fig. 2 where the quantities before and after the impulse have been designated with the subscripts b and a, respectively. Note, as a particular case of the previous conditions, we can obtain the equation for tangential impulse as

$$\text{Ln}\,\mu \pm \frac{z}{v_e} = \text{const.} \tag{21}$$

which is derived from Eq. (20) for $\delta = \theta$ and $\delta = \theta + \pi$, (θ = const), and which applies to forward and retro-tangential impulses [+ and - signs, respectively].

1.1 Coasting Sub-arcs (Zero-thrust)

Along the coasting sub-arcs of the trajectory the well known integrals of the two-body problem are applicable. We will briefly review here these formulas introducing our dimensionless variables. The energy integral and integral of area are respectively written

$$z^2 - \frac{2}{\rho} = H = \text{const.}, \tag{22}$$

$$\rho z \cos\theta = K_1 = \text{const.} \tag{23}$$

The polar equation of the conic section described by the vehicle, with origin at one of its foci is

$$\rho = \frac{K_1^2}{1 + e\cos(\gamma - \omega)} \tag{24}$$

where the eccentricity is

$$e = (1 + K_1^2 H)^{1/2} \quad . \tag{25}$$

For elliptical orbits, ω determines the position of the apsidal line with respect to the inertial system.

From the previous equations one can easily derive that between an initial position 1 and a terminal condition 2 the range (or increment $\Delta\gamma = \gamma_2 - \gamma_1$ of the central angle)

$$\eta = \gamma_2 - \gamma_1 = \arccos f_2 - \arccos f_1 \quad , \tag{26}$$

where

$$f = \frac{\rho (z \cos \theta)^2 - 1}{\left[1 + \rho(z \cos \theta)^2 (\rho z^2 - 2)\right]^{1/2}} \tag{27}$$

2. EQUATIONS OF CONSTRAINT AND OPTIMUM PROBLEM

The problem to be considered in the following is that of optimum transfer of the vehicle from given orbital conditions around the moon to a soft landing on the surface of the moon with minimum fuel expenditure. It is assumed that:

a) The initial orbit (or point on the orbit) is arbitrary,

b) The transfer is effectuated by means of two impulses, the first to de-orbit and the second-on the surface of the moon-to adjust the landing conditions to the specified end-values,

c) The vehicle soft-lands normal to the surface of the moon.

A schematic of the trajectory problem formulated is shown in Figure 3. Since the maneuver involves two impulses, the whole trajectory between the initial (i) and final (f) point may be thought of as a three sub-arcs transfer. That is, the first sub-arc corresponds to the first impulse and takes the vehicle from the initial conditions (i) to conditions (1) at the initiation of the coasting sub-arc. The second sub-arc transfers the vehicle on a coasting flight from conditions (1) to conditions (2). Finally, the third sub-arc is an impulse on the surface of the moon which transfers the vehicle from conditions (2) at the end of the coasting, to the final specified terminal conditions (f).

Using the previous concept and Eqs. (14), (20), (22), (23) and (26) we can obtain the following basic equations of constraint of the problem

$$\varphi_1 \equiv z_i \sin(\delta_1 - \theta_i) - z_1 \sin(\delta_1 - \theta_1) = 0, \tag{28}$$

$$\varphi_2 \equiv \mathrm{Ln}(\mu_i/\mu_1) + \frac{z_i \cos(\delta_1 - \theta_i) - z_1 \cos(\delta_1 - \theta_1)}{v_e} = 0, \tag{29}$$

$$\varphi_3 \equiv z_1^2 - z_2^2 - 2\left(\frac{1}{\rho_1} - \frac{1}{\rho_2}\right) = 0 , \tag{30}$$

$$\varphi_4 \equiv \rho_1 z_1 \cos\theta_1 - \rho_2 z_2 \cos\theta_2 = 0 , \tag{31}$$

$$\varphi_5 \equiv z_2 \sin(\delta_2 - \theta_2) - z_f \sin(\delta_2 - \theta_f) = 0 , \tag{32}$$

$$\varphi_6 \equiv \mathrm{Ln}(\mu_2/\mu_f) + \frac{z_2 \cos(\delta_2 - \theta_2) - z_f \cos(\delta_2 - \theta_f)}{v_e} = 0 , \tag{33}$$

$$\varphi_7 \equiv \eta + f_1 - f_2 = 0, \tag{34}$$

$$\varphi_8 \equiv \rho_i - \rho_1 = 0 , \tag{35}$$

$$\varphi_9 \equiv \rho_2 - \rho_f = 0 , \tag{36}$$

$$\varphi_{10} \equiv \mu_1 - \mu_2 = 0 . \tag{37}$$

According to our previous considerations, we will assume the following set of arbitrary initial and final conditions (in our case the latter will correspond to normal soft landing conditions):

$$\psi_1 \equiv \rho_i - A = 0 , \qquad \psi_2 \equiv z_i - B = 0 ,$$

$$\psi_3 \equiv \theta_i - C = 0 , \qquad \psi_4 \equiv \mu_i - D = 0 ,$$

$$\psi_5 \equiv \rho_f - E = 0 , \qquad \psi_6 \equiv z_f - F = 0 ,$$

$$\psi_7 \equiv \theta_f - H = 0 , \qquad A,B,C,D,E,F,H = \text{given constants.}$$

The equations of constraint and boundary conditions form a set of 17 equations in 19 unknowns. These unknowns are the values of ρ, z, θ and μ at each

of the points i, 1, 2 and f, and the values of η, δ_1 and δ_2. Thus, the problem has two degrees of freedom, and an optimum requirement may be imposed.

Before treating the optimum problem, however, it is convenient to replace the boundary conditions in the equations of constraint in order to reduce the number of variables and equations. Thus, the final set of equations of constraint obtained is

$$\varphi_1 \equiv B \sin(\delta_1 - C) - z_1 \sin(\delta_1 - \theta_1) = 0 , \tag{38}$$

$$\varphi_2 \equiv \mathrm{Ln}\left(\frac{D}{\mu_1}\right) + \frac{B\cos(\delta_1 - C) - z_1 \cos(\delta_1 - \theta_1)}{v_e} = 0 , \tag{39}$$

$$\varphi_3 \equiv z_1^2 - z_2^2 - 2\left(\frac{1}{A} - \frac{1}{E}\right) = z_1^2 - z_2^2 - M = 0 , \tag{40}$$

$$\varphi_4 \equiv A z_1 \cos\theta_1 - E z_2 \cos\theta_2 = 0 , \tag{41}$$

$$\varphi_5 \equiv z_2 \sin(\delta_2 - \theta_2) - F \sin(\delta_2 - H) = 0 , \tag{42}$$

$$\varphi_6 \equiv \mathrm{Ln}\left(\frac{\mu_1}{\mu_f}\right) + \frac{z_2 \cos(\delta_2 - \theta_2) - F\cos(\delta_2 - H)}{v_e} = 0 , \tag{43}$$

$$\varphi_7 \equiv \eta + f_1 - f_2 = 0 , \tag{44}$$

where

$$\left.\begin{aligned} f_1 &= \arccos\left[\frac{A(z_1\cos\theta_1)^2 - 1}{\sqrt{1 + A\left(z_1\cos\theta_1\right)^2 (Az_1^2 - 2)}}\right] , \\ f_2 &= \arccos\left[\frac{E(z_2\cos\theta_2)^2 - 1}{\sqrt{1 + E\left(z_2\cos\theta_2\right)^2 (Ez_2^2 - 2)}}\right] . \end{aligned}\right\} \tag{45}$$

The previous equations form a set of 7 equations in 9 unknowns. The unknowns are: z_1, z_2, θ_1, θ_2, μ_1, μ_f, δ_1, δ_2 and η. The problem thus retains two degrees of freedom, which means that in order to obtain an optimum solution two optimum equations must be added to the previous set. These two equations are derived from the necessary conditions for an extremum, as we will show.

The optimum problem to be considered is therefore stated: "among all solutions satisfying the formulated two-impulse, soft-landing problem find that solution which minimizes the fuel expenditure."

The optimum problem is treated in Section 3.

3. ANALYTICAL TREATMENT OF THE OPTIMUM CONDITIONS

The problem of minimizing the fuel consumption subject to the constraints given by Eqs. (38) to (44) (which embody in themselves the equations of motion and the boundary-conditions), is equivalent to that of maximizing the final mass of the vehicle. Thus, the function to be minimized may be expressed analytically as

$$\Psi = - \mu_f = \text{minimum},$$

since the minimization of $-\mu_f$ is equivalent to maximizing μ_f, (final mass).

To the extent of obtaining the optimum solution, we introduce now a set of undetermined constant Lagrange multipliers λ_j and form the so-called Euler-Lagrange fundamental function:

$$\Lambda = \Psi + \lambda_j \varphi_j \quad , \quad j = 1, \ldots, 7 . \tag{46}$$

If Ψ affords a minimum for any admissible set of differentials dz_1, dz_2, ..., $d\eta$ of the variables of the problem, then the necessary condition for an extremum ($d\Lambda = 0$) requires

$$\frac{\partial \Lambda}{\partial z_1} = \frac{\partial \Lambda}{\partial z_2} = \ldots\ldots = \frac{\partial \Lambda}{\partial \eta} = 0 . \tag{47}$$

Eq. (47) provides 9 equations (known as Euler equations) which together with Eqs. (38) to (44) gives a set of 16 equations in 16 unknowns: $\lambda_1, \ldots, \lambda_7$, z_1, z_2, θ_1, $\theta_2, \ldots\ldots\ldots, \eta$.

3.1 Two Important Optimum Problems - General Set of Euler Equations

From an analytical and practical point of view, two cases are of special interest in the problem we are considering. In fact, since the necessary condition for a minimum is $d\Lambda = 0$, the term associated with the differential of range must vanish, i.e.,

$$\frac{\partial \Lambda}{\partial \eta} d\eta = \left(\Psi_\eta + \lambda_j \frac{\partial \varphi_j}{\partial \eta} \right) d\eta = \lambda_7 \, d\eta = 0. \tag{48}$$

Eq. (48) implies that since no boundary conditions have been imposed on η for the problem formulated in paragraph 2 (i.e., free-range problem), then $d\eta \neq 0$ and consequently $\lambda_7 = 0$. This means that to the extent of treating such problems we can disregard Eq. (44). Thus, we can reduce the formulation of this case to a set of 6 equations in the 8 unknowns: z_1, z_2, θ_1, θ_2, μ_1, μ_f, δ_1 and δ_2, (two-degrees-of-freedom problem).

However, if a boundary condition of the form

$$\Psi_8 \equiv \eta - N = 0, \quad N = \text{const.} \ , \tag{49}$$

is added to the boundary conditions given in paragraph 2 (i.e., given-range problem) then $d\eta = 0$ and $\lambda_7 \neq 0$. In this case, η is no longer a variable of the problem, which now involves a set of 7 equations in 8 unknowns (one-degree-of-freedom problem).

In order to have a general set of Euler equations we will retain Eq. (44) as a constraint with its associated multiplier λ_7. Then, depending on the type of problem we consider, we will set $\lambda_7 = 0$ or $\lambda_7 \neq 0$.

The general set of Euler equations obtained is then

$$\varphi_8 \equiv -\lambda_1 \sin(\delta_1 - \theta_1) - \lambda_2 \frac{\cos(\delta_1-\theta_1)}{v_e} + 2\lambda_3 z_1 + \lambda_4 A\cos\theta_1 - \lambda_7 \frac{2A z_1 \sin\theta_1 \cos\theta_1}{1 + A(z_1\cos\theta_1)^2 (A z_1^2 - 2)} = 0 , \tag{50}$$

$$\varphi_9 \equiv -2\lambda_3 z_2 - \lambda_4 E\cos\theta_2 + \lambda_5 \sin(\delta_2 - \theta_2) + \lambda_6 \frac{\cos(\delta_2 - \theta_2)}{v_e} + \lambda_7 \frac{2E z_2 \sin\theta_2 \cos\theta_2}{1 + E(z_2\cos\theta_2)^2 (E z_2^2 - 2)} = 0 , \tag{51}$$

$$\varphi_{10} \equiv \lambda_1 \cos(\delta_1 - \theta_1) - \lambda_2 \frac{\sin(\delta_1 - \theta_1)}{v_e} - \lambda_4 A \sin\theta_1 + \lambda_7 \frac{Az_1\left[1 + \cos^2\theta_1 (Az_1^2 - 2)\right]}{1 + A(z_1\cos\theta_1)^2 (Az_1^2 - 2)} = 0 , \tag{52}$$

$$\varphi_{11} \equiv \lambda_4 E \sin\theta_2 - \lambda_5 \cos(\delta_2 - \theta_2) + \lambda_6 \frac{\sin(\delta_2 - \theta_2)}{v_e} - \lambda_7 \frac{E z_2\left[1 + \cos^2\theta_2 (E z_2^2 - 2)\right]}{1 + E(z_2\cos\theta_2)^2 (E z_2^2 - 2)} = 0 , \tag{53}$$

$$\varphi_{12} \equiv -\lambda_2 + \lambda_6 = 0 , \tag{54}$$

$$\varphi_{13} \equiv 1 + \frac{\lambda_6}{\mu_f} = 0 , \tag{55}$$

$$\varphi_{14} \equiv \lambda_1\left[B\cos(\delta_1 - C) - z_1\cos(\delta_1 - \theta_1)\right] + \lambda_2 \frac{z_1 \sin(\delta_1 - \theta_1) - B\sin(\delta_1 - C)}{v_e} = 0, \tag{56}$$

$$\varphi_{15} \equiv \lambda_5\left[z_2\cos(\delta_2-\theta_2)-F\cos(\delta_2-H)\right]+\lambda_6\frac{F\sin(\delta_2-H)-z_2\sin(\delta_2-\theta_2)}{v_e}=0. \tag{57}$$

The solution of this set of Euler equations will be considered in Section 4.

4. OPTIMUM CONDITIONS FOR FREE-RANGE PROBLEMS

As shown before, in Eqs. (50) to (57) $\lambda_7 = 0$. Furthermore, Eqs. (38) and (42) show that the second term in the left-hand member of both Eqs. (56) and (57) vanish. Thus, in view of Eqs. (39) and (43), a simple physical reasoning indicates that Eqs. (56) and (57) can only be satisfied with

$$\lambda_1 = \lambda_5 = 0 \ . \tag{58}$$

Eqs. (54) and (55) readily lead to

$$\lambda_2 = \lambda_6 = -\mu_f \ . \tag{59}$$

Replacing the previous conditions in Eq. (53) we can derive

$$\lambda_4 = \frac{\mu_f \sin(\delta_2-\theta_2)}{E\, v_e \sin\theta_2} \ . \tag{60}$$

Eqs. (58) to (60) replaced in Eq. (52) provide the following first necessary equation for an optimum:

$$E\sin\theta_2\sin(\delta_1-\theta_1)-A\sin\theta_1\sin(\delta_2-\theta_2)=0 \tag{61}$$

From Eqs. (50) and (51) we can derive

$$\lambda_3=\frac{-\lambda_4 A\cos\theta_1+\lambda_2\frac{\cos(\delta_1-\theta_1)}{v_e}}{z_1}=\frac{-\lambda_4 E\cos\theta_2+\lambda_6\frac{\cos(\delta_2-\theta_2)}{v_e}}{z_2},$$

which after introducing Eqs. (59) , (60) and (61) leads to the second necessary condition for an optimum:

$$\sin(\delta_1 - \theta_1)\left(E z_1 \cos\theta_2 - A z_2 \cos\theta_1\right) + A \sin\theta_1\left[z_1 \cos(\delta_2 - \theta_2) - z_2 \cos(\delta_1 - \theta_1)\right] = 0. \tag{62}$$

Eqs. (61) and (62) are the two necessary optimum equations which added to Eqs. (38) to (44) form a determined optimum set of 9 equations in the 9 unknowns: z_1, z_2, θ_1, θ_2, μ_1, μ_f, δ_1, δ_2 and η. Using this set of equations we can obtain an optimum condition expressed only in terms of the variables at point 1, after the first impulse. This expression is of practical value for the numerical solution of the problem.

In fact, from Eqs. (38), (40), (41) and (61) one can derive, respectively

$$\sin(\delta_1 - \theta_1) = \frac{B \sin(\delta_1 - C)}{z_1} , \tag{63}$$

$$z_2 = \sqrt{z_1^2 - M} , \tag{64}$$

$$\sin\theta_2 = \sqrt{1 - \left(\frac{A}{E}\right)^2 \frac{z_1^2 \cos^2\theta_1}{z_1^2 - M}} \tag{65}$$

$$\sin(\delta_2 - \theta_2) = \frac{E \sin(\delta_1 - \theta_1)}{A \sin\theta_1} \sqrt{1 - \left(\frac{A}{E}\right)^2 \frac{z_1^2 \cos^2\theta_1}{z_1^2 - M}} \tag{66}$$

The expressions for $\cos\theta_2$ and $\cos(\delta_2 - \theta_2)$ follow easily from the previous equations. Thus, replacing these expressions in Eq. (62) and performing extensive manipulations we can derive the following necessary condition:

$$\Omega \equiv \left[M \cos\theta_1 \sin(\delta_1 - \theta_1) - (z_1^2 - M) \sin\theta_1 \cos(\delta_1 - \theta_1)\right]^2 + z_1^2 \left\{(M - z_1^2)\sin^2\theta_1 + \left[\frac{E}{A}\sin(\delta_1 - \theta_1)\right]^2 \left[z_1^2 - M - \left(\frac{A z_1 \cos\theta_1}{E}\right)^2\right]\right\} = 0 . \tag{67}$$

Simple geometrical considerations derived from Fig. 2 and our developments in paragraph 1 show that

$$\tan \delta_1 = \frac{z_1 \sin \theta_1 - B \sin C}{z_1 \cos \theta_1 - B \cos C} \quad , \tag{68}$$

and, consequently, Eqs. (67) and (68) implicitly express the optimum condition in Eq. (67) as a function of the form

$$\Omega = \Omega(z_1, \theta_1) \quad . \tag{69}$$

5. OPTIMUM CONDITION FOR GIVEN-RANGE PROBLEMS

In this case, a boundary condition of the form given in Eq. (49), is assumed imposed. Therefore, our problem is formulated in terms of 7 equations i.e., Eqs. (38) to (44) in 8 unknowns; z_1, z_2, θ_1, θ_2, μ_1, μ_f, δ_1 and δ_2. This is a one degree of freedom problem in which, as discussed in paragraph 3.1, $\lambda_7 \neq 0$. The necessary optimum equation which saturates this degree of freedom may be derived from the Euler equations. In order to present the equations in a more compact form, we will introduce the following notation:

$$f = \arccos \left[\frac{\rho(z \cos\theta)^2 - 1}{\sqrt{1 + \rho(z\cos\theta)^2(\rho z^2 - 2)}} \right] , \tag{70}$$

$$\frac{\partial f}{\partial z} = f_z = - \frac{2\rho z \sin\theta \cos\theta}{1 + \rho(z\cos\theta)^2(\rho z^2 - 2)} \quad , \tag{71}$$

$$\frac{\partial f}{\partial \theta} = f_\theta = \frac{\rho z^2 \left[1 + \cos^2\theta(\rho z^2 - 2)\right]}{1 + \rho(z\cos\theta)^2(\rho z^2 - 2)} \quad . \tag{72}$$

Note that in this problem, as in the previous case,

$$\lambda_1 = \lambda_5 = 0 \quad , \tag{73}$$

$$\lambda_2 = \lambda_6 = -\mu_f \ . \tag{74}$$

Thus, introducing these replacements in Eqs. (52) and (53) we obtain a set of two algebraic, nonhomogeneous equations in λ_4 and λ_7. From these equations we can derive

$$\lambda_4 = \frac{\mu_f}{v_e}\left[\frac{f_{\theta_1}\sin(\delta_2-\theta_2) - f_{\theta_2}\sin(\delta_1-\theta_1)}{E\sin\theta_2 f_{\theta_1} - A\sin\theta_1 f_{\theta_2}}\right] , \tag{75}$$

$$\lambda_7 = \frac{\mu_f}{v_e}\left[\frac{A\sin\theta_1\sin(\delta_2-\theta_2) - E\sin\theta_2\sin(\delta_1-\theta_1)}{E\sin\theta_2 f_{\theta_1} - A\sin\theta_1 f_{\theta_2}}\right] , \tag{76}$$

where the subindex of f_θ (and f_z in the following) indicates the point at which the function is evaluated.

From Eqs. (50) and (51), after eliminating λ_3, we now obtain

$$\frac{\mu_f}{v_e}\left[z_1\cos(\delta_2-\theta_2) - z_2\cos(\delta_1-\theta_1)\right] + \lambda_4(E z_1\cos\theta_2 - A z_2\cos\theta_1) + \\ + \lambda_7(z_1 f_{z_2} - z_2 f_{z_1}) = 0 \ . \tag{77}$$

Finally, introducing Eqs. (75) and (76) in Eq. (77), and rearranging, it follows that

$$(E\sin\theta_2 f_{\theta_1} - A\sin\theta_1 f_{\theta_2})\left[z_1\cos(\delta_2-\theta_2) - z_2\cos(\delta_1-\theta_1\right] + \\ + (E z_1\cos\theta_2 - A z_2\cos\theta_1)\left[f_{\theta_1}\sin(\delta_2-\theta_2) - f_{\theta_2}\sin(\delta_1-\theta_1)\right] + \\ + (z_1 f_{z_2} - z_2 f_{z_1})\left[A\sin\theta_1\sin(\delta_2-\theta_2) - E\sin\theta_2\sin(\delta_1-\theta_1)\right] = 0 \ . \tag{78}$$

Eq. (78) provides the necessary condition for an optimum which together with Eqs. (38) to (44) suffices to determine the minimizing trajectory for given range. As in the previous problem, to the extent of the numerical solution of this case, it is convenient to express Eq. (78) in terms of the variables at point 1 (beginning of the coasting sub-arc). For this, we can use the following expressions derived from previous equations:

$$z_2 = \sqrt{z_1^2 - M} \quad , \tag{79}$$

$$\sin(\delta_2 - \theta_2) = \frac{F \sin(\delta_2 - H)}{\sqrt{z_1^2 - M}} \quad , \tag{80}$$

$$\cos \theta_2 = \frac{A z_1 \cos \theta_1}{E \sqrt{z_1^2 - M}} \quad , \tag{81}$$

$$\delta_2 = \arctan \left[\frac{F + z_2 \sin \theta_2}{z_2 \cos \theta_2} \right] \quad , \quad (\text{for } \theta_f = -\pi/2) \quad , \tag{82}$$

Eqs. (78) to (82) implicitly express the necessary condition for an optimum in terms of the variables z_1 and θ_1.

6. GENERAL CONSIDERATION ON THE NUMERICAL SOLUTION OF THE PREVIOUS PROBLEMS

The numerical solution of the problems previously considered appears somewhat complicated due to the form of the equations for an optimum obtained and the transcendental character of these expressions. However, such difficulties may be easily resolved based on the analysis of the impulse conditions presented in paragraph 1 and basic geometrical relations implied by such developments. This permits us to develop a technique of numerical solution based on a one-dimensional search of the values of z_1 and θ_1 which satisfy the optimum equations [Eqs. (67) and (78)]. Once these values are determined we can obtain the rest of the optimum values along the trajectory without difficulty, as will be shown in the following.

From our analysis in paragraph 1 we find that is convenient to introduce the angle

$$\alpha = \arctan\left[\frac{z_i \sin(\theta_1 - \theta_i)}{z_1 - z_i \cos(\theta_1 - \theta_i)}\right] \tag{83}$$

Using this angle and simple geometrical relations we can determine the angle of orientation of the first impulse (δ_1). In fact, for

$$\left.\begin{aligned} &\text{a)}\ z_1 - z_i \cos(\theta_1 - \theta_i) < 0 \ , \quad \delta_1 = \pi + \theta_1 + \alpha \ , \\ &\text{b)}\ z_1 - z_i \cos(\theta_1 - \theta_i) = 0 \ , \quad \delta_1 = \theta_1 + \frac{\pi}{2} \ , \\ &\text{c)}\ z_1 - z_i \cos(\theta_1 - \theta_i) > 0 \ , \quad \delta_1 = \theta_1 + \alpha \ . \end{aligned}\right\} \tag{84}$$

Thus, α is obtained from Eq. (83) as a function of the boundary conditions $z_i = B$, $\theta_i = C$, and the variables z_1 and θ_1. Knowing the optimum set (z_1, θ_1), satisfying Eqs. (67) and (78), we can then find the optimum direction of the impulse δ_1. A graphical representation of the case $z_1 - z_i \cos(\theta_1 - \theta_i) > 0$ is shown in Fig. 4.

In Fig. 5 we show the cases of impulse with initial angle of attitude negative (i.e., $\theta_i < 0$ in Fig. 5.A) and impulse with initial angle of attitude positive (i.e., $\theta_i > 0$ in Fig. 5.B). In constructing these figures we have assumed that z_i, θ_i and θ_1 are known. In other words, we assume that the direction θ_1 of the vector velocity after the impulse is known, but its magnitude is not. If we now assume that z_1 may take all the possible values $0 \leqq z_1 \leqq \infty$, we can determine the angular sector (shadowed in Fig. 5) within which the angle δ_1 of the impulse must lie for such fixed θ_1 and any z_1. This construction is of practical value in order to have a simple geometrical way of verifying the numerical computations of δ_1. Furthermore, and principally, it provides a graphical interpretation of the method of numerical solution followed in order to organize a systematic one-dimensional search of the values of z_1 and θ_1 which satisfy Eqs. (67) and (78).

The method of solution followed in order to determine $z_{1_{opt.}}$, $\theta_{1_{opt.}}$ $\delta_{1_{opt.}}$ is shown graphically in Fig. 6. The values of z_i and θ_i are given by the boundary conditions. We then assume a given θ_1 and let z_1 take different values z_{11}, z_{12}, z_{13}, etc., as shown in Fig. 6. For each value of z_1 assumed, there is a corresponding value for δ_1. These values are called δ_{11}, δ_{12} and δ_{13} in Fig. 6 and are numerically computed using Eqs. (83) and (84). These values are then replaced in Eqs. (67) and (78) to verify whether they are satisfied or not. Numerical applications show that the solution is unique. Thus, there is only one set satisfying Eqs. (67) and (78).

The values of the variables at the point 2 (end of the coasting sub-arc) can be readily computed from the equations of motion as a function of the values at point 1, as shown in previous paragraphs. Furthermore, since the coasting transfer orbit must hit the surface of the moon at point 2 (or at least graze it so the boundary condition $\rho_f = \rho_2 = \rho_{moon} = E$ is satisfied), then it must be $-\frac{\pi}{2} < \theta_2 \leqq 0$. And, moreover, since for a soft-landing $z_f < z_2$, then we obtain (similar to the first impulse)

$$\left.\begin{aligned} &\text{for:}\quad z_f - z_2 \cos(\theta_f - \theta_2) < 0\ , \quad \delta_2 = \theta_f + \pi + \alpha = \frac{\pi}{2} + \alpha\ , \\ &\text{for:}\quad z_f - z_2 \cos(\theta_f - \theta_2) > 0\ , \quad \delta_2 = \theta_f + \alpha\ , \end{aligned}\right\} \tag{85}$$

$$\alpha = \arctan\left[\frac{z_2 \sin(\theta_f - \theta_2)}{z_f - z_2 \cos(\theta_f - \theta_2)}\right]. \tag{86}$$

A graphical representation of the conditions before and after the second impulse is shown in Fig. 7.

Thus, once the values $\rho_1 = \rho_i$, z_1, θ_1 and δ_1 are determined, the values $\rho_2 = \rho_f$, z_2, θ_2 and δ_2 may be easily computed. All these values are used to compute Eqs. (61), (62) and (67) or Eq. (78) -- depending on whether we are dealing with a free-range or a given-range problem -- and thus verify if the necessary equations for an optimum are satisfied. The total propellant expenditure is computed from

$$\mu_{prop.} = 1 - \exp. \left[\frac{B \cos(\delta_1 - C) + z_2 \cos(\delta_2 - \theta_2) - z_1 \cos(\delta_1 - \theta_1) - F \cos(\delta_2 - H)}{v_e} \right] , \tag{87}$$

which derives from Eqs. (39) and (43) for $\mu_i = D = 1$.

The procedure of numerical solution outlined, based on a one-dimensional search of the optimum values, may be easily programmed for automatic computation since it involves simple calculations of algebraic expressions. In these expressions the difficulties associated with the possible multiple values of the trigonometric functions have now been removed using simple geometrical and analytical considerations which derive from the impulse conditions previously studied.

In our analysis we have assumed that the n-dimensional space of admissible solutions defined by the variables of the problem is unbounded. However, the requirements that the coasting transfer between the points 1 and 2 be elliptical and hit the surface of the moon implies certain inequality constraints that bound the domain of admissible solutions. Consequently, should one encounter a solution in common with the boundaries, it is convenient to compute the fuel consumption for some admissible trajectories near the boundaries, interior to the admissible domain, in order to verify the actual character of the optimum solutions on the boundary. In our problem the inequality constraints imposed result as a consequence of the fact that the coasting transfer is elliptical and that it must hit, or at least graze, the surface of the moon. Thus, such conditions require the satisfaction of the following inequalities

$$z_1^2 - \frac{2}{\rho_i} < 0 , \tag{88}$$

$$\frac{-1 + \sqrt{1 + \left(z_1^2 - \frac{2}{\rho_i}\right)\left(\rho_i z_1 \cos \theta_1\right)^2}}{z_1^2 - \frac{2}{\rho_i}} \leqq 1 . \tag{89}$$

When Eq. (89) is satisfied with the equal sign the transfer coasting sub-arc grazes the surface of the moon, and if it is larger than one the transfer does not hit the moon. The solution with the equal sign identified the limiting, grazing solution. These inequality constraints can easily be incorporated in the program of numerical computation described before since they are only functions of z_1 and θ_1. As the practice has shown, the introduction of these inequality constraints expedites the procedure of solution since they permit us to eliminate several cases from consideration. Thus, the computational work required to obtain the optimum values of z_1, θ_1 and δ_1 is substantially reduced.

7. BASIC CHARACTERISTICS OF THE LANDING TRAJECTORIES - NUMERICAL APPLICATIONS

Based on the scheme of numerical solution previously discussed, several applications have been conducted. In order to analyze different cases involving an angle of attitude $\theta_i = 0$, $\theta_i > 0$ and $\theta_i < 0$, the initial point assumed in each case has been located on a given elliptical orbit around the moon. Thus, all the optimum landing trajectories considered start from the same elliptical initial orbit. This will permit us to study each case individually and at the same time compare all the optimums in order to determine the absolute optimum. The most convenient point to start the landing maneuver from an elliptical orbit will be thus determined.

The arbitrary initial orbit assumed has a dimensionless semi-major axis $a = 2.25$ and an eccentricity $e = 0.3333$. Consequently, the dimensionless radius of the apogee is $\rho_{ap.} = 3$ and the radius of the perigee is $\rho_{per.} = 1.5$. The corresponding velocities at apogee and perigee are $z_{ap.} = 0.4714$ and $z_{per.} = 0.9428$, respectively. The reference velocity used in these computations is the satellite velocity on the surface of the moon, $V_R = 5,420$ ft/sec. and the reference radius is the radius of the moon, $r_M = 938.54$ n. miles. The landing velocity assumed is $z_f = 0.00184$, which corresponds to 10 ft/sec and the landing is normal, i.e., $\theta_f = -\pi/2$.

7.1 Analytical Considerations on the Free-Range Optimum Trajectories

In the following we will discuss free-range problems.

We observe that if the first impulse corresponds with a tangential forward or retro-thrust, then $\theta_1 = \theta_i$ and $\delta_1 = \theta_1$ or $\delta_1 = \pi + \theta_1$. Thus, $\sin(\delta_1 - \theta_1) = 0$ and either $\theta_1 = 0$ or $\theta_1 \neq 0$. In the first case, obviously $\sin(\delta_1 - \theta_1) = 0$ and $\theta_1 = 0$ satisfy both necessary conditions in Eqs. (61) and (62). In the second case, replacing $\sin(\delta_1 - \theta_1) = 0$ and $\sin\theta_1 \neq 0$ in Eq. (67) we obtain $M z_2^2 \sin^2\theta_1 = 0$, which therefore is not satisfied because $M \neq 0$ and $z_2 \neq 0$. Thus, the previous considerations lead to the conclusion that an optimum landing with initial tangential thrust can only occur for $\theta_1 = \theta_i = 0$, i.e., at the apogee or perigee of the initial elliptical orbit. If $\theta_i \neq 0$ (that is, at points of the initial elliptical orbit other than its apogee or perigee), no tangential thrust is admissible for an optimum solution and therefore $\sin(\delta_1 - \theta_1) \neq 0$. In such case, the minimizing trajectory which satisfies Eqs. (61) and (62) is obtained following the method of numerical solution indicated in paragraph 6 and discussed in detail in paragraph 7.2.

In order to study the characteristics of the landing trajectory starting at the apogee of the initial orbit with a retro-impulse, we notice that from Eqs. (61) and (62) we can obtain

$$\sin(\delta_2 - \theta_2)(E z_1 \cos\theta_2 - A z_2 \cos\theta_1) + E \sin\theta_2 \left[z_1 \cos(\delta_2 - \theta_2) - z_2 \cos(\delta_1 - \theta_1) \right] = 0. \tag{90}$$

Eqs. (62) and (90) imply Eq. (61) [which is precisely the necessary condition for a non-trivial solution $(E z_1 \cos\theta_2 - A z_2 \cos\theta_1) = 0$, $z_1 \cos(\delta_2 - \theta_2) - z_2 \cos(\delta_1 - \theta_1) = 0$]. Thus, Eqs. (62) and (90) can be used as the set of necessary conditions for a free-range optimum, instead of Eqs. (61) and (62).

The transfer orbit starting at apogee with a retro-thrust (i.e., $\theta_1 = \theta_i = 0$, $\delta_1 = \pi$) obviously satisfied Eq. (62) since $\sin(\delta_1 - \theta_1) = 0$ and $\sin\theta_1 = 0$. Also, regarding the landing conditions, $\sin\theta_2 = 0$ and $\sin(\delta_2 - \theta_2) = 0$ obviously satisfy Eq. (90). Thus a Hohmann type transfer would satisfy both necessary conditions. However, in view of the final boundary conditions imposed (i.e., $z_f \neq 0$, $\theta_f \neq 0$), such transfer is not admissible due to the fact that $\sin(\delta_2 - \theta_2) = 0$

implies a terminal tangential thrust which can not satisfy the end-values specified. Thus a Hohmann type transfer (i.e., transfer with $\theta_1 = \theta_2 = 0$) does not satisfy the necessary conditions for an optimum derived. Consequently, at point 2 (see Fig. 3) the orbit starting at the apogee (or perigee) of the initial orbit with a tangential thrust must have $\theta_2 \neq 0$. Numerical solutions have shown that $\theta_2 < 0$, and in our case very small, so the transfer orbit results close to a Hohmann transfer. Due to these facts (i.e., $\theta_2 < 0$, and small) the angle of direction of the second impulse results $\delta_2 \approx \pi$, (see Fig. 7).

The optimum landing trajectories starting at points on the initial ellipse other than its apogee or perigee (i.e., $\theta_i \neq 0$) can not follow a Hohmann type transfer (viz., a transfer with $\theta_2 = 0$). This is due to the fact that, since $\sin(\delta_1 - \theta_1) \neq 0$ and $\sin \theta_1 \neq 0$, then if $\theta_2 = 0$, Eq. (61) leads to the condition $\delta_2 = 0$ or $\delta_2 = \pi$ (tangential forward or retro-thrust). Again, as before, none of these solutions can satisfy the specified terminal condition $\theta_f = -\frac{\pi}{2}$. Thus, $\theta_2 \neq 0$. In general, the numerical solutions obtained show that $\theta_2 < 0$. Its magnitude, depends on the characteristics of the initial orbit. In our applications θ_2 is very small.

7.2 Results of Numerical Solutions

Several minimum fuel consumption solutions starting at different points of the initial elliptical orbit assumed were computed. The absolute minimum fuel consumption was obtained for a landing trajectory starting at the apogee of the initial orbit. The fuel consumption in our application was 57.7% of the initial total weight of the vehicle. The maximum fuel consumption, among all the minimum fuel trajectories starting at different points on the initial ellipse, was obtained for that one starting at the perigee of the initial orbit. In general, the difference in fuel consumption between these two cases depends on the eccentricity of the initial orbit. Thus, in our case, due to the low eccentricity of the initial orbit assumed the perigee solution required only 5% more fuel than the apogee solution.

The minimum fuel consumption trajectories starting at a radius $\rho_i = 2.8$ are shown in Figs. 8 and 9. The first corresponds to $\theta_i > 0$ and the second to $\theta_i < 0$. As can be seen in these figures the solutions obtained

are grazing trajectories, almost tangent to the surface of the moon at the landing point. In both cases the fuel consumption is the same (as it is for all other optimum trajectories starting from the same elliptical orbit, at the same radius, but with different initial angle of attitude). The trajectory starting with $\theta_i > 0$ gives larger range than the one starting with $\theta_i < 0$.

The procedure of numerical solution followed was described in paragraph 6 and numerical results are presented in Figs. 10 and 11. These figures show the results obtained for different landing trajectories starting from the initial elliptical orbit at a radius $\rho_i = 1.9$ and at an angle of attitude $\theta_i = -17.5^\circ$. All these trajectories satisfy the same terminal conditions. As indicated before, we take an arbitrary direction θ_1 and vary z_1 searching for a solution of Eq. (67). The values of z_1 searched have an upper bound determined by the constraints in Eqs. (88) and (89). For each z_1 (and a given θ_1) the value of δ_1 is obtained from Eq. (68), or Eqs. (83) and (84). These values of z_1, δ_1 and θ_1 are replaced in Eq. (67). The set which satisfied that equation is used to compute θ_2, z_2 and the second impulse direction δ_2, which satisfy the terminal landing conditions $\theta_f = -\pi/2$, $z_f = 0.00184$. For this we use Eqs. (79), (81) and (82) [or Eqs. (85) and (86)]. The propellant expenditure is obtained from Eq. (87).

The previous search was done rapidly by means of a computer program specifically designed to be fully automatic.

To the extent of determining the character of the solutions obtained and identify the optimum solution we introduced a function Λ which is the square root of the sum of the squares of Eqs. (61) and (62). Λ vanishes only when both equations vanish, thus identifying the optimum solution.

The numerical solutions shown in Figs. 10 and 11 exhibit the results obtained for the case considered. Note that the constraints in Eqs. (88) and (89), limit the range of possible solutions, (i.e., $-170^\circ \leqq \theta_1 \leqq -19^\circ$. Fig. 10 shows that Λ vanishes for $\theta_1 = -19^\circ$, thus determining the optimum orbit. Also, it shows that for a given initial radius the optimum solution is unique. Since $\theta_i = -17.5^\circ$, we see that the optimum angle ($\theta_1 = -19^\circ$) is very close to the initial angle. However, they can not be equal since no solution is

admissible with tangential thrust (i.e., for $\theta_1 = \theta_i$). This can be seen in Fig. 10 and was demonstrated in paragraph 7.1.

Fig. 11 shows the final mass of the vehicle as a function of θ_1. In general, Fig. 11 appears to indicate that the extremum -- for the case considered -- is not too sensitive to variations in θ_1 (and consequently z_1 and δ_1). Note that an error $\Delta\theta_1 = -10^\circ$ with respect to the optimum θ_1, would cause an extra expenditure of only about 5% of fuel, in order to land the vehicle along a non-optimum, admissible trajectory, satisfying the same boundary values.

7.3 Given-Range Optimum Solution

The given-range optimum trajectories may be obtained following a numerical search similar to that described for free-range problems in paragraph 7.2. In this case, the optimum condition to be satisfied is given by Eq. (78). Using Eqs. (79) to (82) and (83) to (86), we can apply a one-dimensional search of z_1 for each given θ_1, in order to determine the set satisfying Eq. (78) and the range condition imposed. An example of the minimum fuel solution starting at a radius $\rho_i = 2.8$ ($\theta_i < 0$) on the initial orbit and giving a range $\eta = 57^\circ$, is shown in Fig. 12. The optimum equation for given-range problems Eq. (78), confirms our considerations in paragraph 7.1 regarding the non-admissibility of Hohmann type transfers, for landings starting at the apogee or perigee of the initial orbit with tangential impulses. In fact, for the same range and boundary-conditions, the given-range and free-range optimum trajectories must be the same. Thus, if the Homann transfer is optimum for the free-range problem it should be optimum for the problem with given-range $\eta = \pi$. However, in such case, $\theta_1 = \theta_2 = 0$, $\delta_1 = \pi$, and $\delta_2 \neq 0$, in order to satisfy the end-conditions. Thus, Eq. (78) leads to

$$\frac{\left(E z_1 - A z_2\right) A z_1^2 \left(A z_1^2 - 1\right)}{1 + A z_1^2 \left(A z_1^2 - 2\right)} \sin \delta_2 = 0 \ . \qquad (91)$$

Eq. (91) is satisfied for $\delta_2 = 0$, which is not compatible with the end-values imposed, for $A z_1 - 1 = 0$, which implies a circular transfer orbit thus not

admissible, and for $E\, z_1 - A\, z_2 = 0$, which is not admissible by virtue of Eq. (31). Thus, these considerations confirm the non-admissibility of Homann type transfers in the case considered.

Similarly, for problems in which $\sin(\delta_1 - \theta_1) \neq 0$ and $\sin \theta_1 \neq 0$, (i.e., for transfer orbits starting at points other than the apogee or perigee of the initial orbit), the free-range solution satisfied the given-range solution for the same range and boundary conditions. In both cases the resulting optimum trajectory is the same. Thus, since the free-range solution satisfies Eqs. (61), (62) and (90), then the same solution must satisfy Eq. (78). This can easily be seen writing Eq. (78) in the form

$$f_{\theta_1}\left\{E \sin\theta_2\left[z_1 \cos(\delta_2 - \theta_2) - z_2 \cos(\delta_1 - \theta_1)\right] + \sin(\delta_2 - \theta_2)(E\, z_1 \cos\theta_2 - A\, z_2 \cos\theta_1)\right\}$$

$$- f_{\theta_2}\left\{A \sin\theta_1\left[z_1 \cos(\delta_2 - \theta_2) - z_2 \cos(\delta_1 - \theta_1)\right] + \sin(\delta_1 - \theta_1)(E\, z_1 \cos\theta_2 - A\, z_2 \cos\theta_1)\right\}$$

$$- \left(z_1 f_{z_2} - z_2 f_{z_1}\right)\left[E \sin\theta_2 \sin(\delta_1 - \theta_1) - A \sin\theta_1 \sin(\delta_2 - \theta_2)\right] = 0 . \qquad (92)$$

Eq. (92) contains Eqs. (61), (62) and (90) in its terms. Thus, <u>for the same range</u>, the free-range trajectory obviously satisfies the necessary condition of the given-range problem. However, for the same boundary-value problem the solution of the given-range problem, with <u>arbitrarily specified range</u>, is no longer satisfied by the free-range solution. This is due to the fact that, for given-range problems, in general, each term of Eq. (92) does not necessarily vanish as it is required by the solution of the free-range problem.

ACKNOWLEDGMENTS

The author is indebted to Mr. Octavio Winter for his collaboration in programming the numerical applications.

REFERENCES

1. R. Courant and D. Hilbert, "Methods of Mathematical Physics," Vols. I and II, New York, Interscience Publishers, Inc., 1953 and 1962, respectively.

2. C. R. Cavoti, "Extremal Arcs and Approximate Impulsive Solutions in an Inverse Square Field," Space Sciences Lab. paper, General Electric Co., Contract NAS 8-11040, George C. Marshall, Space Flight Center, N.A.S.A., Huntsville, Alabama, May 1964.

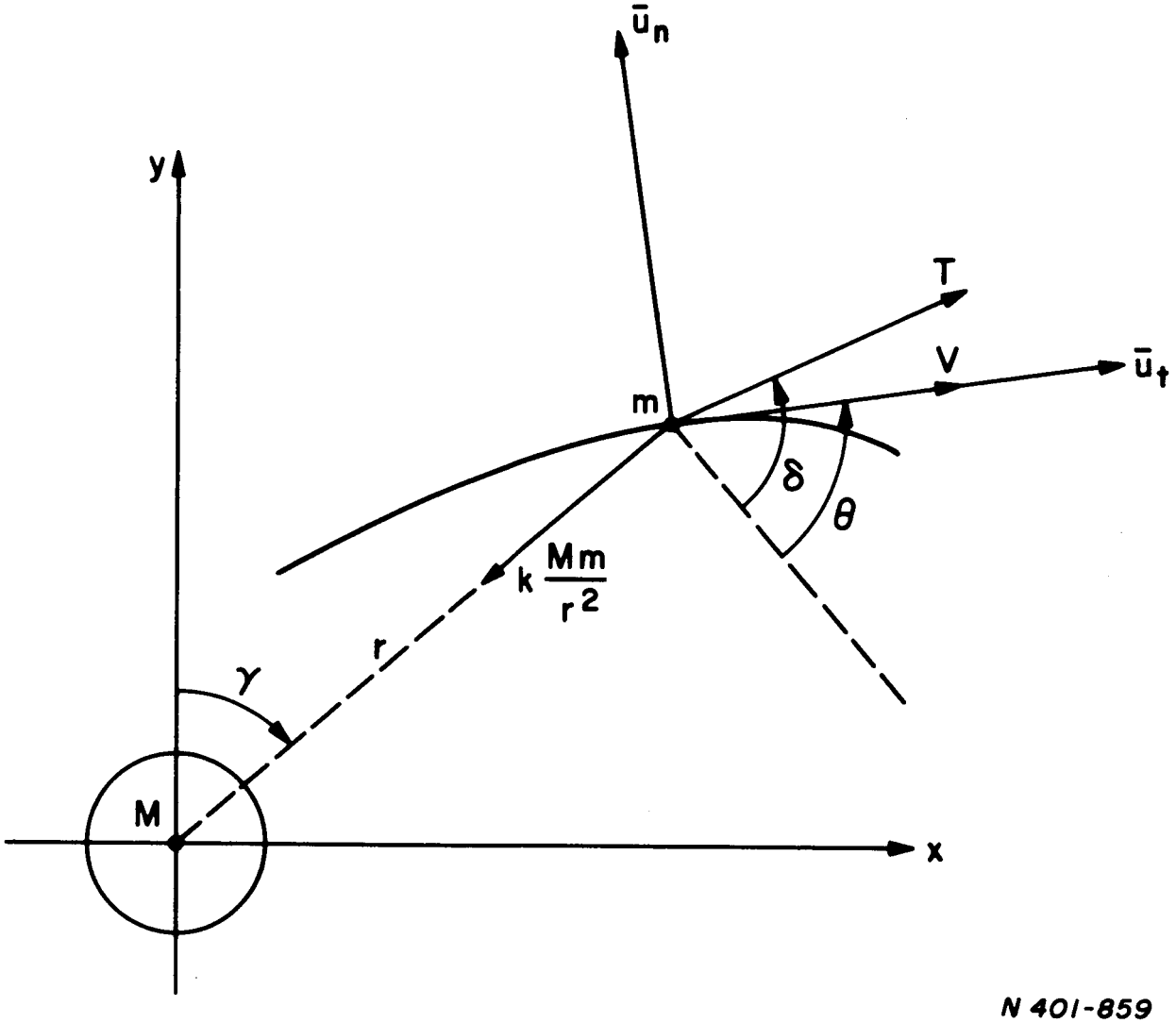

Figure 1. Reference Systems, Angles, and Forces Acting on the Vehicle.

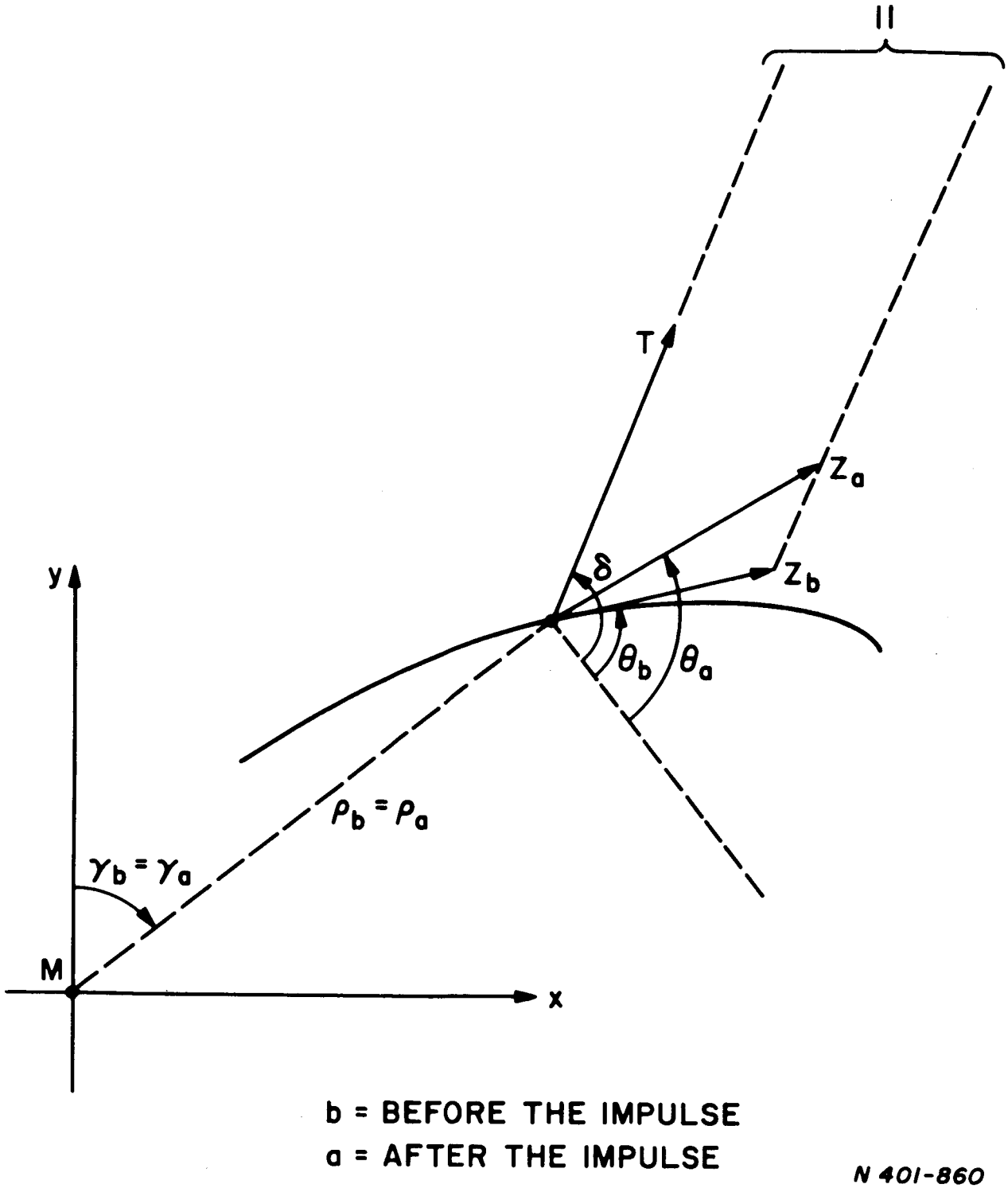

Figure 2. Conditions Before and After the Impulse.

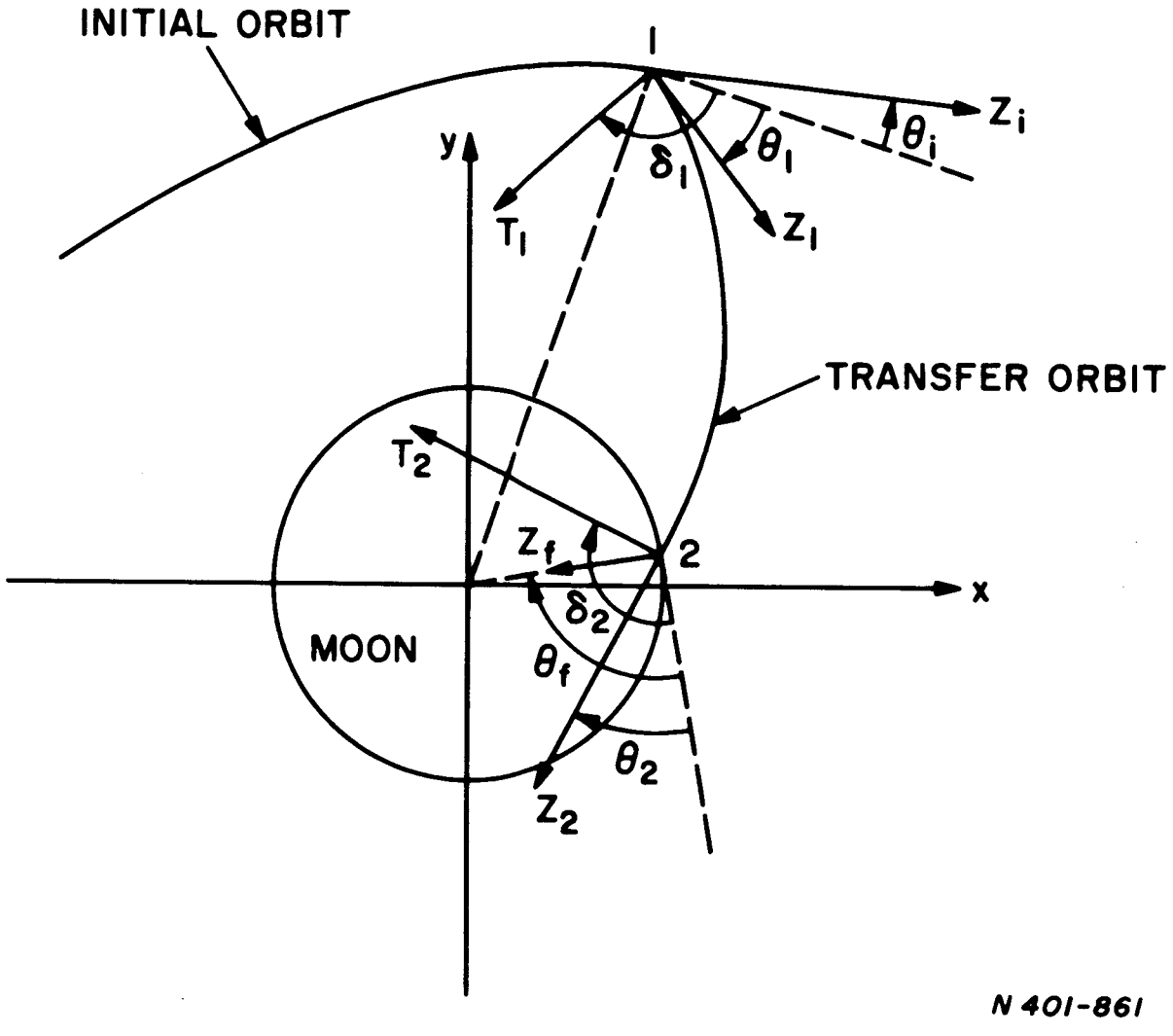

Figure 3. Characteristics of the Landing Trajectories Considered.

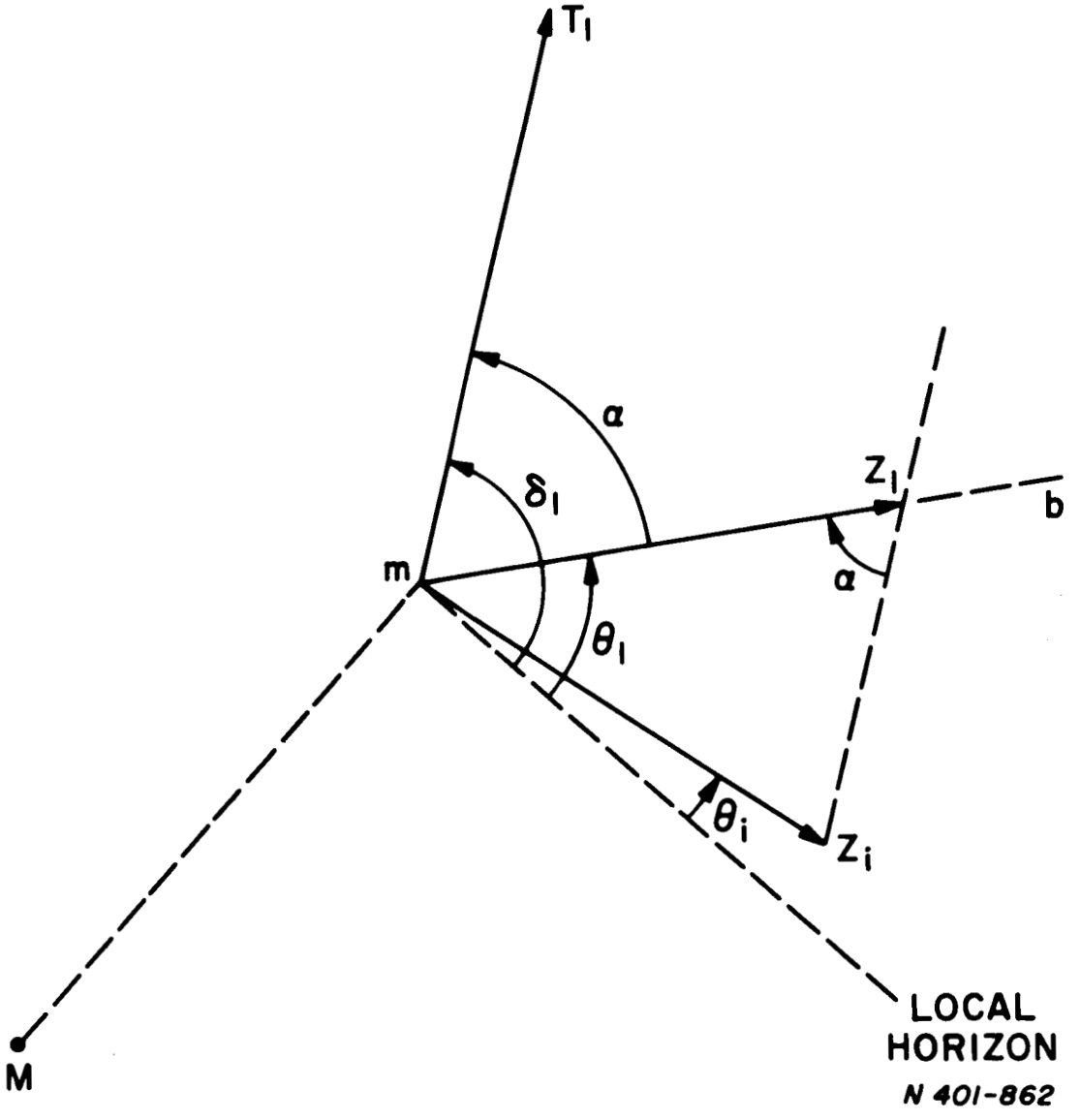

Figure 4. Geometry of the Impulse.

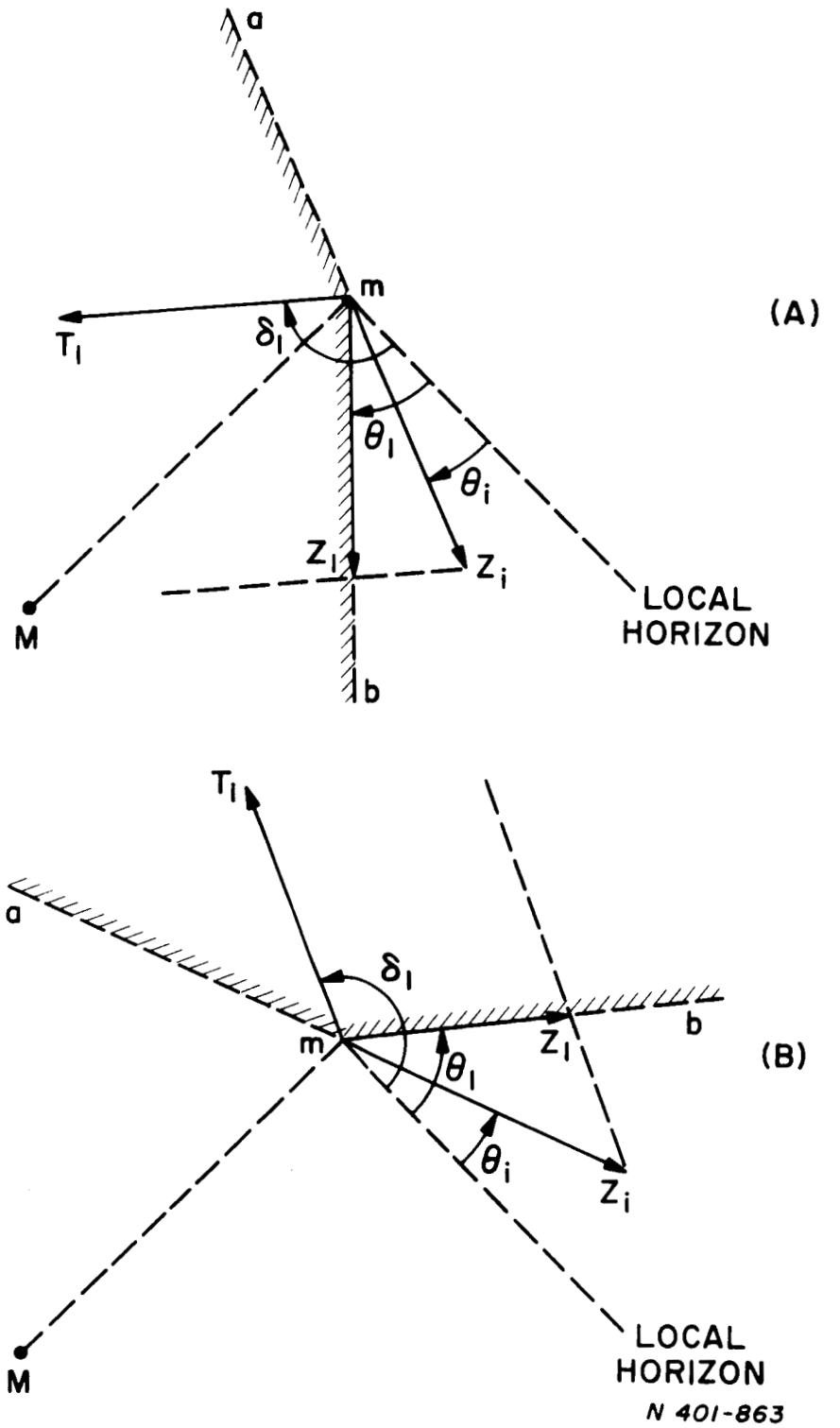

Figure 5. Impulses with $\theta_i < 0$ and $\theta_i > 0$.

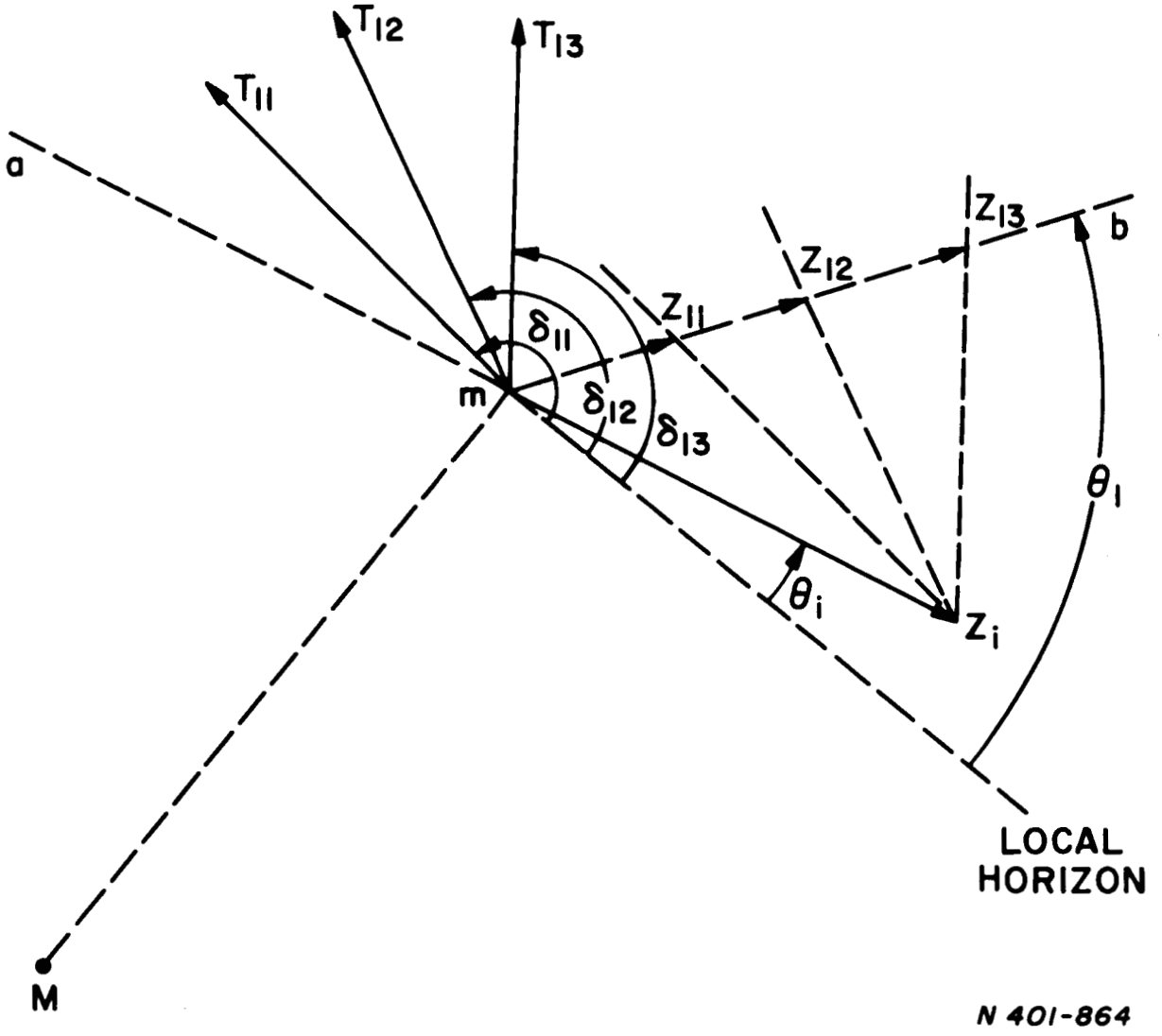

Figure 6. Direction of the Impulse for Given θ_i, θ_1 and Variable z_1.

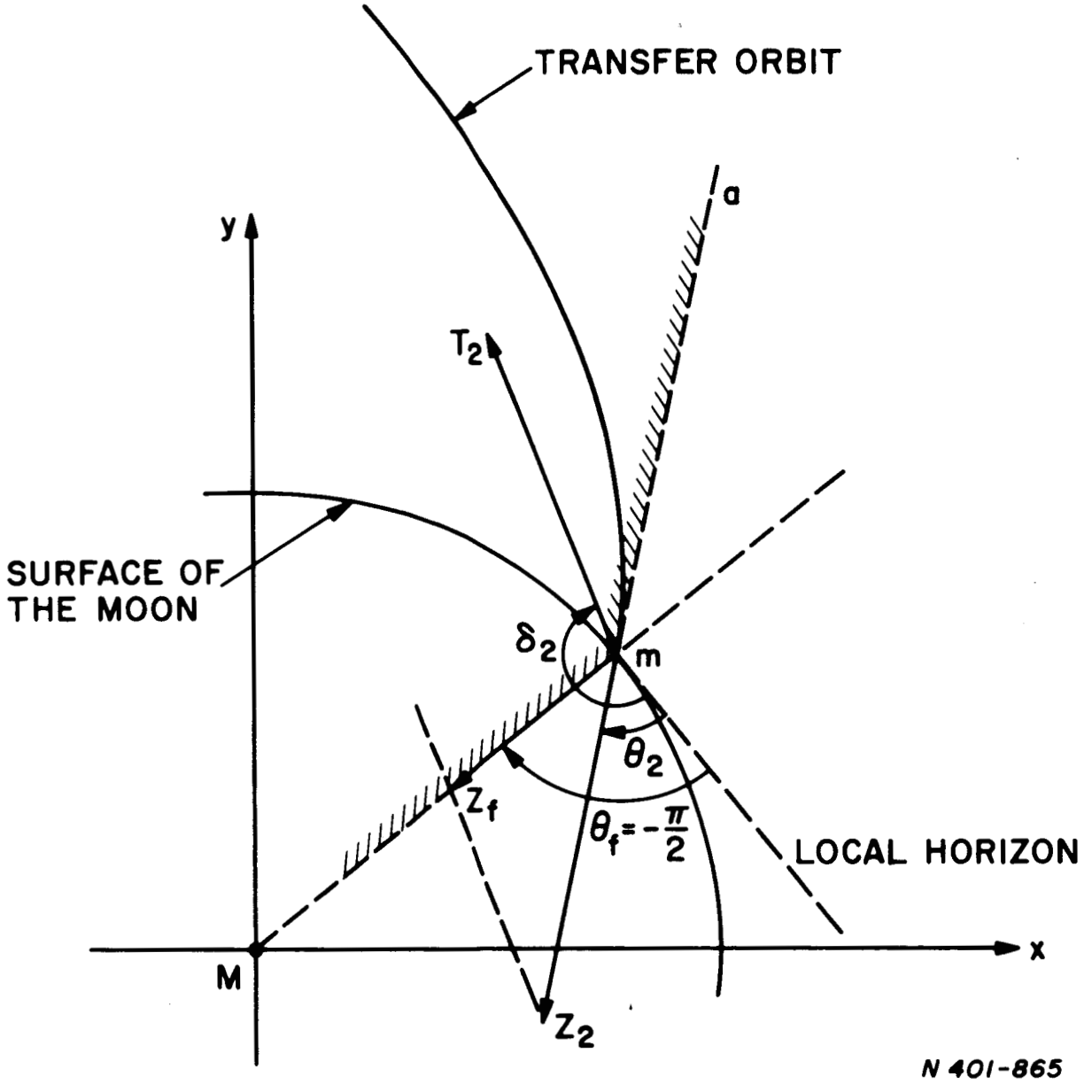

Figure 7. Geometry of the Lunar Landing.

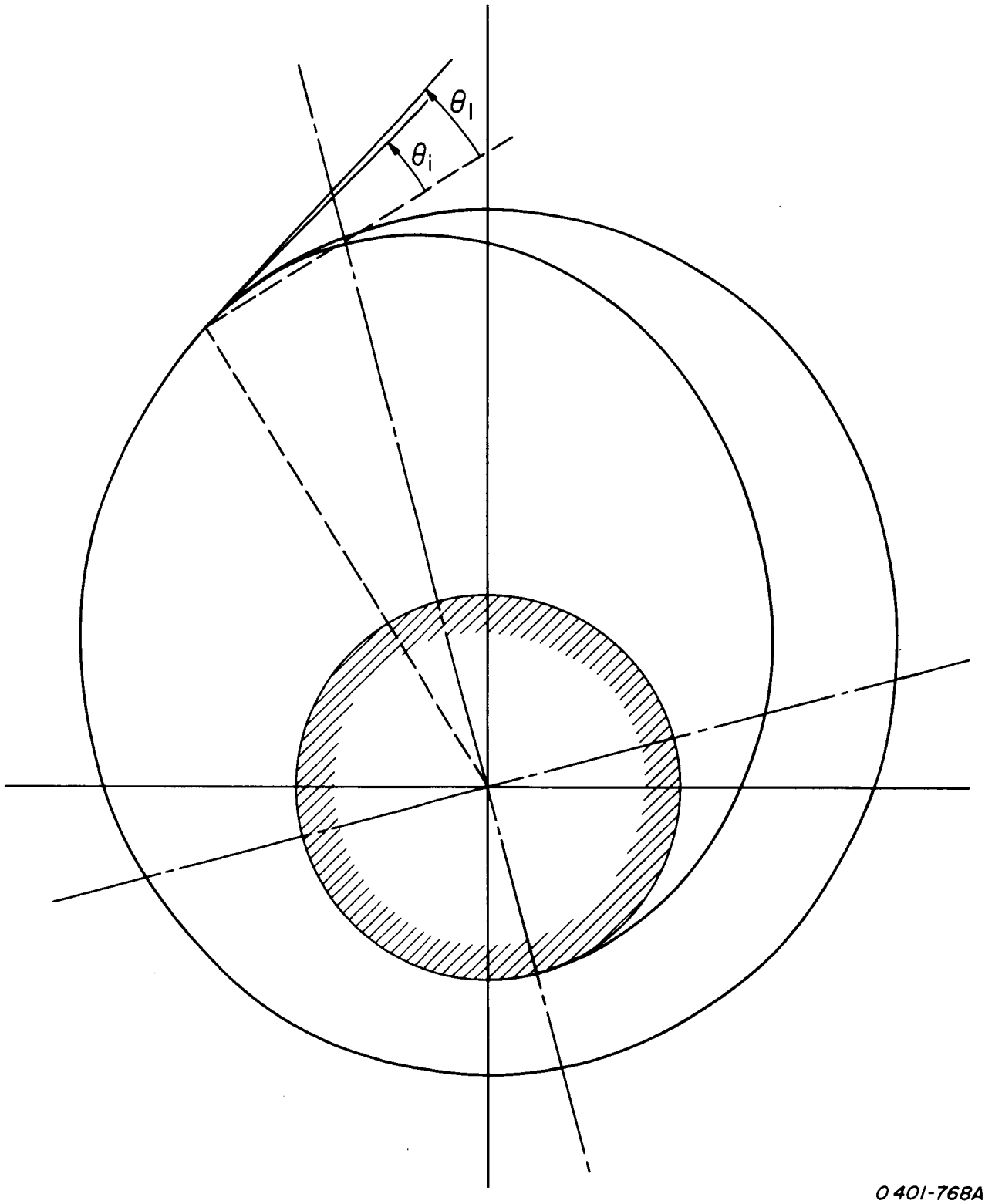

Figure 8. Minimum Fuel Consumption Landing for $\rho_i = 2.8$ and Free-Range (Case $\theta_i > 0$).

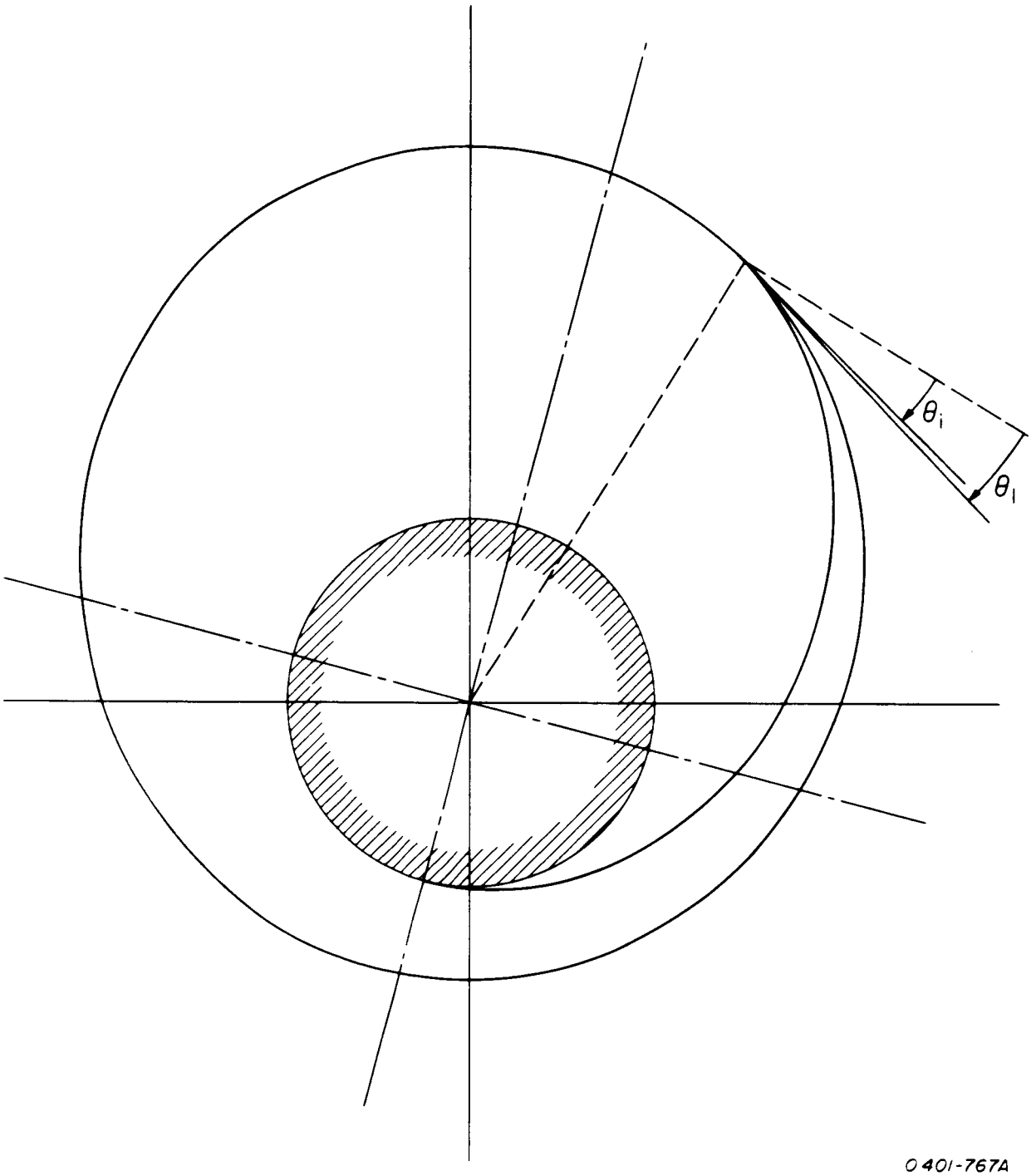

Figure 9. Minimum Fuel Consumption Landing for $\theta_i = 2.8$ and Free-Range (Case $\theta_i < 0$).

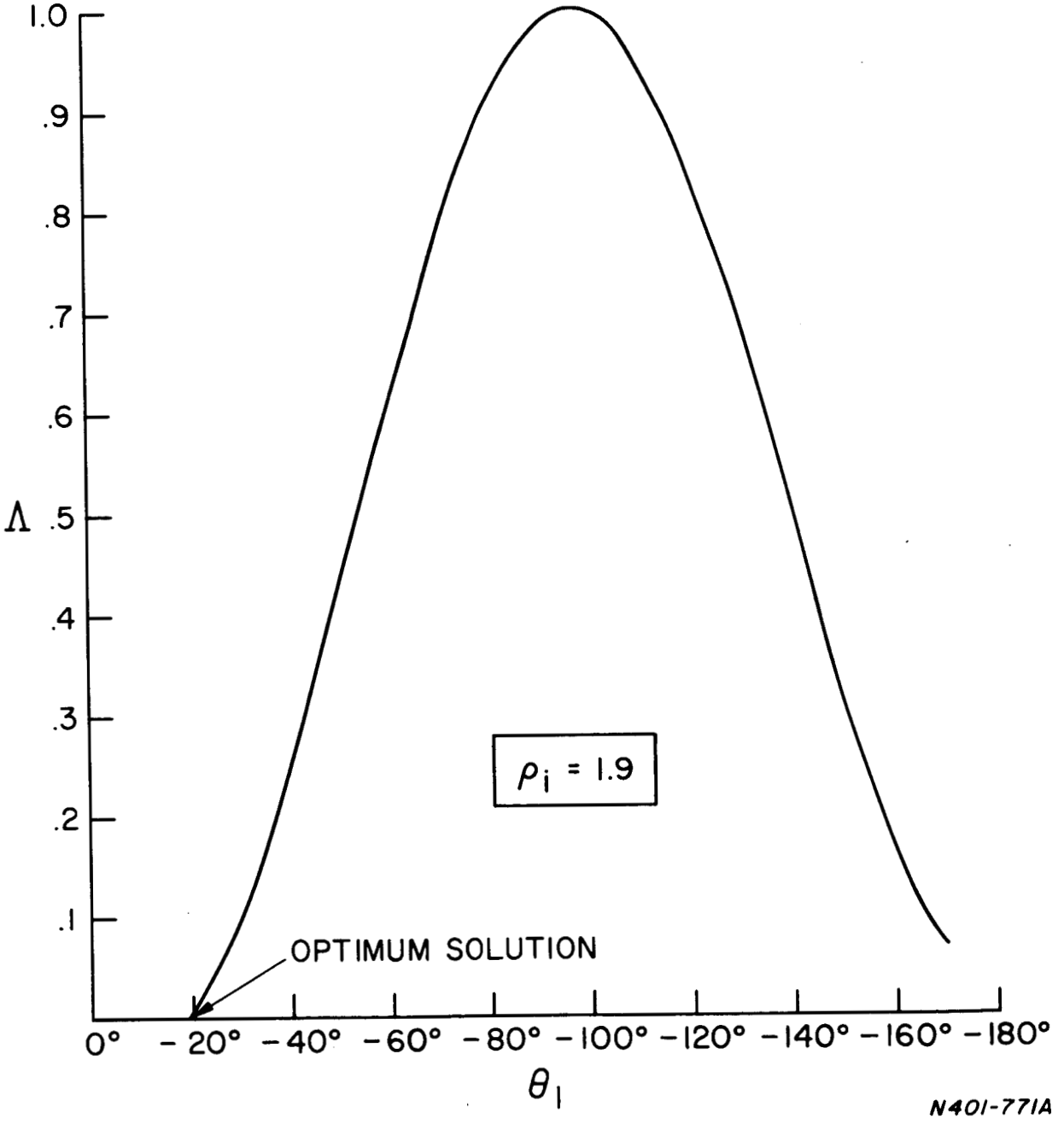

Figure 10. Λ - Function for $\rho_i = 1.9$ and Variable θ_1.

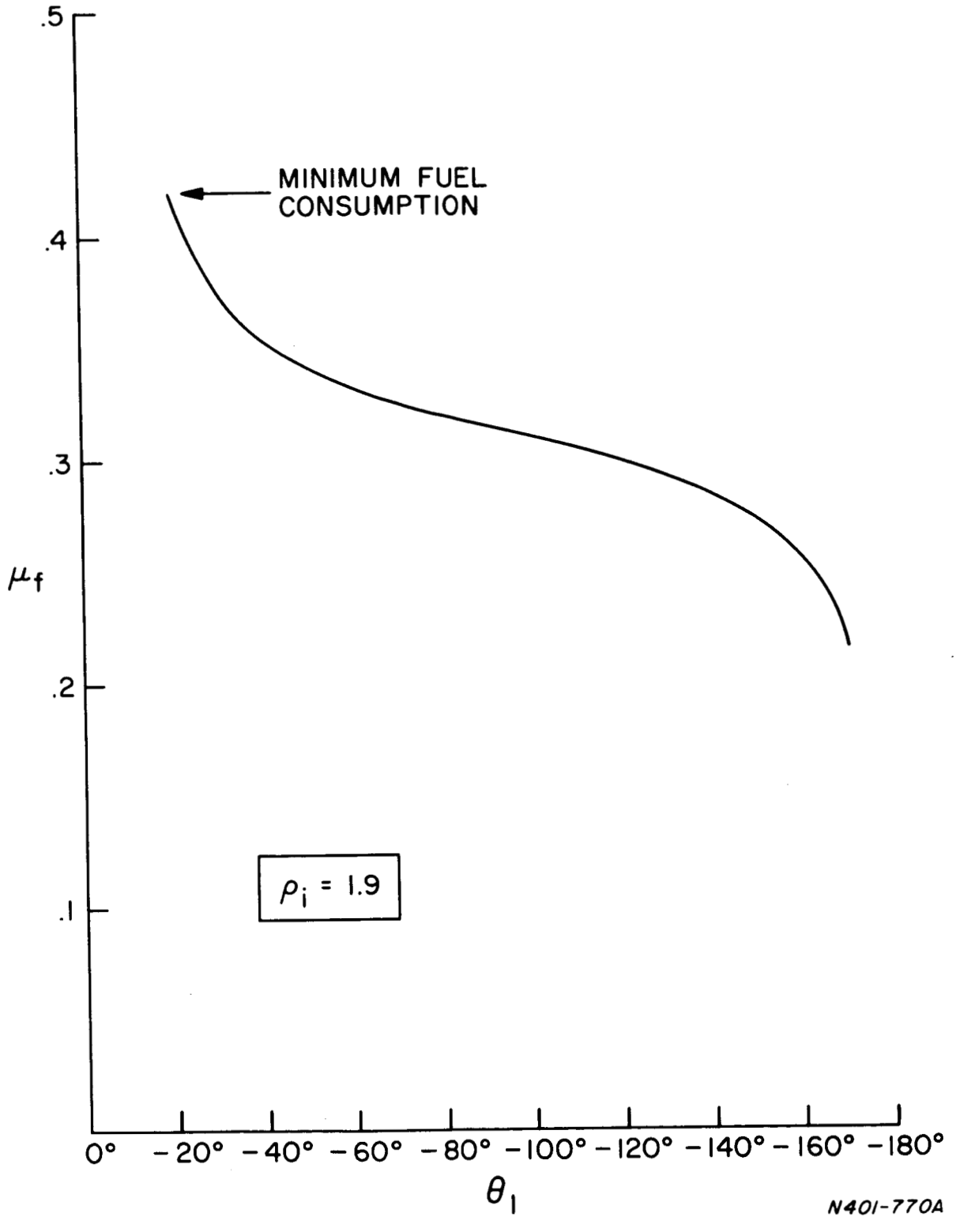

Figure 11. Final Mass for ρ_i = 1.9 and Variable θ_1.

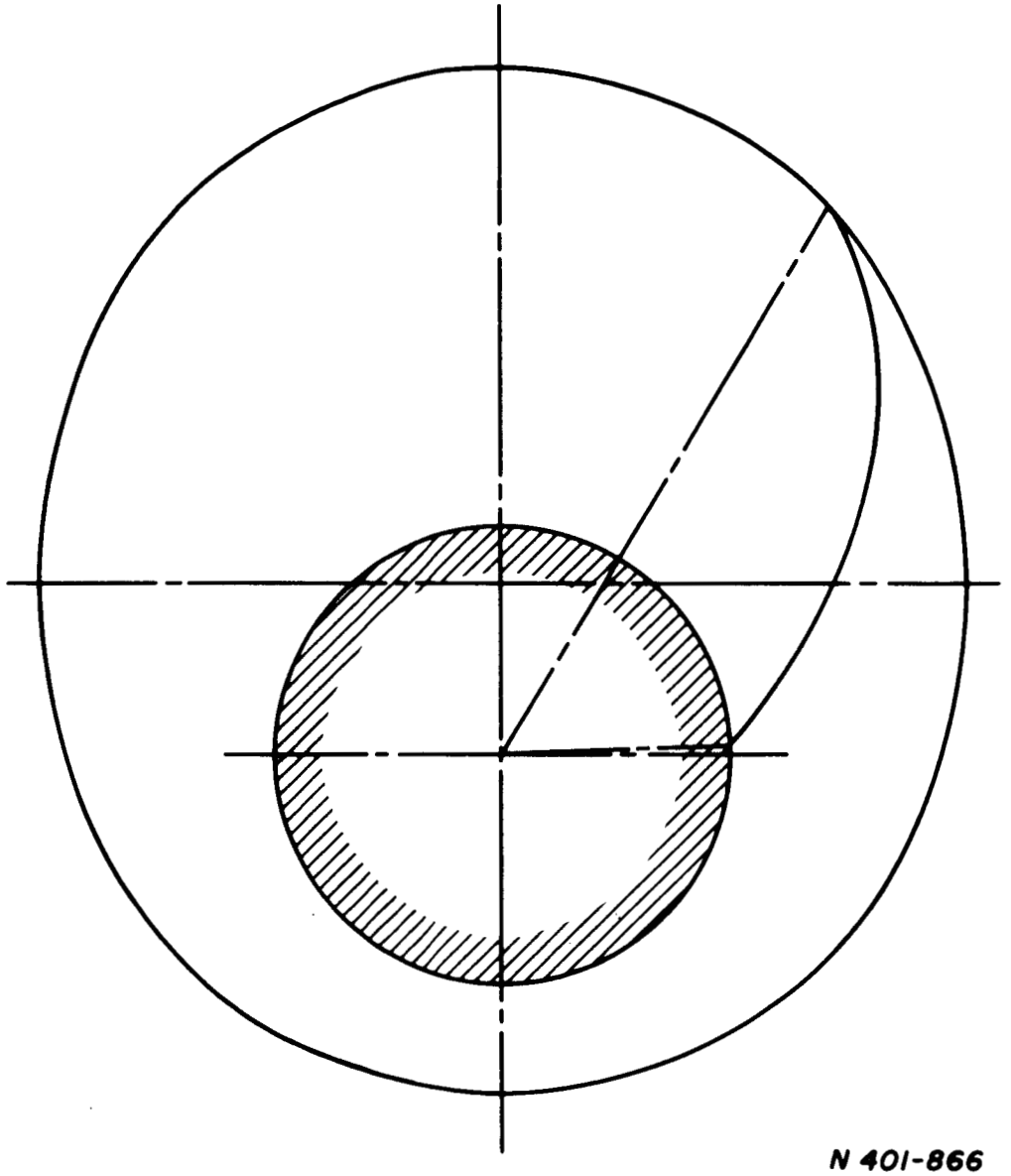

Figure 12. Minimum Fuel Consumption Landing for $\rho_i = 2.8$ and Range $\eta = 57^{\circ}$.